

Design and Development of DC-DC Boost Converter based on DSP TMS320F2812 for PV Application

Mohammed Rasheed, Rosli Omar and Marizan Sulaiman

Faculty of Electrical Engineering, Universiti Teknikal Malaysia Melaka, Industrial Power, Hang Tuah Jaya, Durian Tunggal, Melaka - 76100, Malaysia;
mohamed_tchno@yahoo.com, rosliomar@utem.edu.my, marizan@utem.edu.my

Abstract

Objective: In this paper, we reported experiment control voltage signal of Pulse Width Modulation (PWM) design circuit of closed loop implemented of dc-dc boost converter for application Photovoltaic (PV) simulator. **Methods/Statistical Analysis:** In this design, the converter provides step-up voltage from the PV generating systems as an interface between the load and PV panel and let the follow-up of the **Findings:** The operation was performed based on a specifically associated converter to the PV panel which is controlled via the observed P&O and Maximum Power Point Tracking (MPPT) perturb. The regulation is achieved by PWM at a fixed frequency and the switching device is generally Insulated Gate Bipolar Transistor IGBT. **Application/Improvements:** The feedback path is established with a control circuit such that a proper duty cycle is achieved for the desired output voltage (V_o) for the application photovoltaic generating systems. The proposed scheme is modelled to utilise MATLAB/SIMULINK and verified through simulation result, and prototype experiment for the purpose of utilising the Digital signal processing (DSP) TMS320F2812 control PWM.

Keywords: Converters DC/DC, Digital Signal Processing TMS320F2812, Maximum Power Point Tracking Pulse Width Modulation

1. Introduction

A dc-dc converter increases or decreases dc voltage, which is widely used in the regulated switch-mode dc power supplies. In the dc motor drive application, it can be considered equivalent to an Ac transformer with a continuously variable-turns ratio¹⁻³ Like a transformer, it is meant to convert step-up boost converter or step-down buck converter of a dc source⁴. The defy in the high applications of energy renewable is concise to generate the future non-isolated high step-up DC/DC boost converter⁵. The model of switching for the boost converter can be utilised as a regulated and unregulated to convert an output dc voltage as a regulated⁶⁻⁷. The normally achieved regulations are via (PWM) at a constant frequency and the general switching devices are BJT, MOSFET or IGBT⁸⁻⁹⁻¹⁰. Moreover, the minimum oscillator frequency should be about 100 times longer than the transistor switching time to maximize efficiency. As the switching

loss is due to the transistor limitation, a boost converter consists of a diode, inductor, fully controlled transistor, capacitor, and load¹¹⁻¹². Meanwhile, an inductor considers the main components of a boost converter, a high-frequency switch, and a diode. An analysis assumes a closed loop by using the (PID) controller feedback with the PWM control circuit such that it is achieved for the desired output voltage (V_o)¹³⁻¹⁴⁻¹⁵. The proposed scheme is modelled to utilise MATLAB/SIMULINK and verified through simulation result and prototype experiment aims to utilise the (DSP) TMS320F2812 control PWM. The feedback path was established by controlling (MPPT) perturb and observing P&O circuit such that a proper duty cycle was achieved for the desired output voltage (V_o) for the application of PV system.

2. Photovoltaic System PV

PVs are used to create power by utilizing the sunlight

photonic. The photoelectric impact was initially depicted by a French physicist, Edmund Becquerel, in 1839¹⁶. PV systems have an essential application in remote areas which are not able to connect the power grid. For instance, the stand-alone power system solar provides power for lighting, pump water, electrified livestock fencing, and refrigeration of vaccines, telecommunications, and many other forms of life support in rural area⁹. A stand-alone PV system can be split into the grid-connected system. PV system comprises of three sections; the first is module or solar panels (solar irradiation energy to electric energy), while the second is interface part or desire power section, to manage and induce electric energy obtained from PV system which is a proportion designed to the need of consumer and the third one is load power as shown in Figure 1. Figure 2. presents the equivalent circuit diagram to a PV cell corresponding to Equation 2¹⁷.

$$I_{pv} = I_p - I_D - I_{sh} \tag{1}$$

$$= I_p - I_o \left[e^{\frac{q(V_{pv} + R_s I_{pv})}{nKT}} - 1 \right] - \frac{V_{pv} + R_s I_{pv}}{R_{sh}} \tag{2}$$

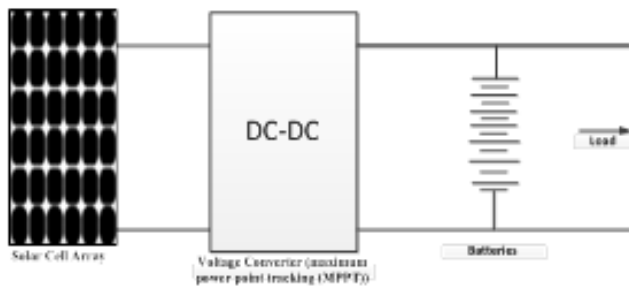


Figure 1. PV power system diagram.

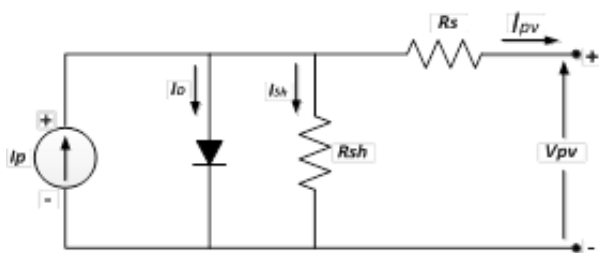


Figure 2. Equivalent circuit diagram of a PV cell.

Where I_p = Photo current (A) V_{pv} = Terminal voltage (V) I_D = Diode Current (A) I_o = Saturation current (A) I_{sh} = Shunt current (A) N = Ideality factor q = Electron charge (C) D = Constant R_s = Series resistance (Ω) R_{sh} = Shunt resistance

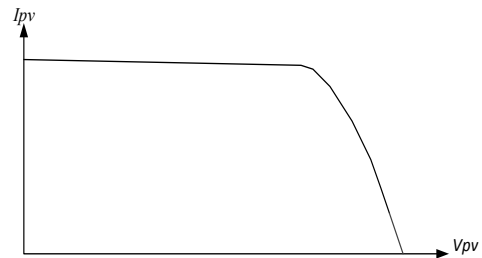


Figure 3. I-V Curve for Solar cell.

In Figure 3, the operating characteristic I_{PV} - V_{PV} of a solar cell¹⁶. The PV array comprises of various PV cells individuals that are connected together to get a unit with a power suitable rating. The PV array characteristic can be a specific connected parallel via the number of cells via the multiplied voltage of an individual cell. Three important operating points are SCC, OCV, and MPP.

2.1 Open Circuit Voltage OCV

At the voltage in Figure 4, the operating point A is the OCV. Figure 5. shows the current open circuit condition with obsolete which is clarified by Equation 4.

$$I_p - I_o \left[e^{\frac{qV_{oc}}{nKT}} - 1 \right] = 0 \tag{3}$$

$$V_{oc} = \frac{nKT}{q} \ln \left[\frac{I_p + I_o}{I_o} \right] \tag{4}$$

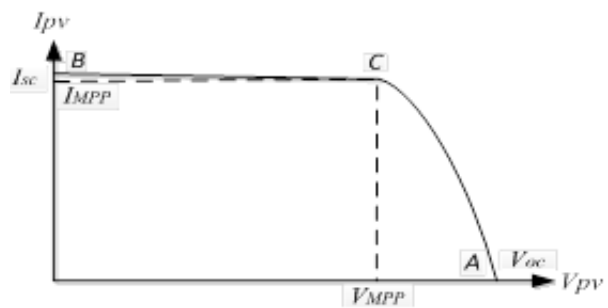


Figure 4. I-V curve of a solar cell.

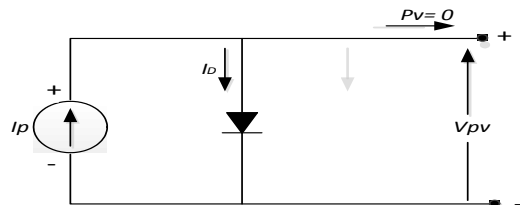


Figure 5. Equivalent circuit during open circuit condition.

2.2 Short Circuit Current SCC

At the current, point P operating in Figure 6. is the SCC. Figure 6 shows the short circuit with the obsolete resistance series R_s in Equation 5.

$$I_{sc} = I_p \tag{5}$$

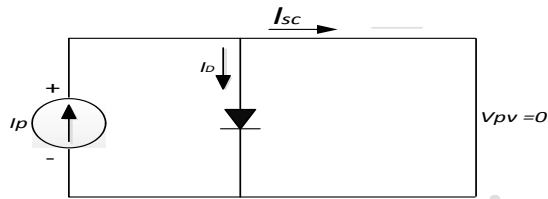


Figure 6. Equivalent circuit during short circuit condition.

2.3 Maximum Power Point MPP

Under the temperature cell and constant irradiance, the curve I-V for characteristics determine the operating point for intersection of a PV array. The curve I-V for characteristic shows where the inclination M equals to 1 of the (MPP) in Figure 7. Hence, the angle of the inclination β is 45. Mathematically for the current-voltage, the second derivative functions in respect to the voltage results for the function power-voltage. Power is maximum at the MPP, hence, the inclination of the power-voltage angle = 0 and the gradient curve is also = 0¹⁸.

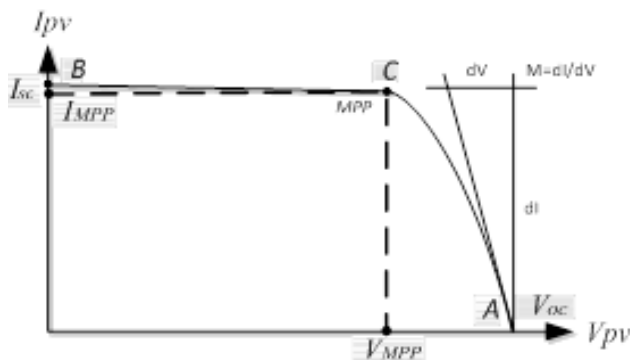


Figure 7. Curve I-V characteristic for (MPP).

3. Dc-Dc Boost Converter

The boost converter popular is non isolated for power topology stage, infrequently called a step-up voltage-current stage. The power supply configuration selects the boost power stage in order to require the greater output than the input voltage. The input current for a boost power

stage is permanent, or non-pulsating because the output diode is conducted only during a part of the switching cycle. The output capacitor supplies the complete load current for the rest of the switching cycle. Figure 8. shows a simplified schematic of the boost converter power stage.

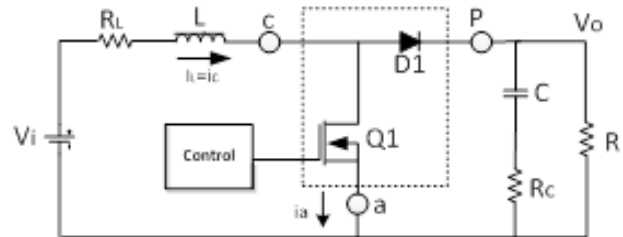


Figure 8. Boost power stage schematic.

Inductor L and capacitor C are not at all like buck converter, where peak-to-peak output voltage ripple is dependent on L . The inductor dc resistance, R_L , is incorporated into the investigation and capacitor equivalent series resistance (ESR). Meanwhile, RC represents R resistor of the load seen by the output power supply. A power stage operating can be in the discontinuous or continuous inductor current mode. In the LI continuous mode, the current flows constantly in the L during the entire switching cycle in a steady-state operation. On the other hand, in the LI discontinuous mode the LI is zero for a part of the switching cycle. It obtains peak value at zero, and returns to zero during each switching cycle. For a power stage, it is attractive to stay in one mode over its expected operating conditions because the power stage frequency response changes significantly between the two operating modes. In the (CCM), the power is transferred from source to load utilizing a 2- stage process. When switch 'S' is turned on, the inductor stores the energy power which equivalent circuit is appeared in Figure 9.

$$\Delta i_c = d_c \% * T * \frac{V_s}{L} \tag{6}$$

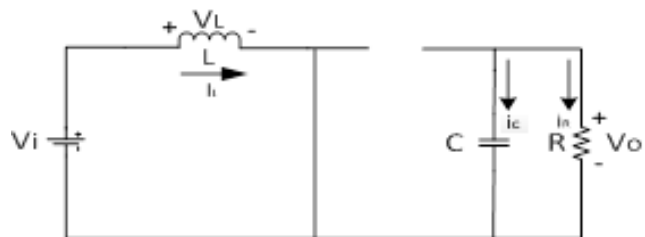


Figure 9. ON State circuit diagram.

For the turned OFF switch 'S', the energy power is stored in the inductor and the provided energy power is transferred to the load via the diode as shown in Figure 10¹⁵.

$$\Delta i_o = [(1 - d)_c \%] * T * \frac{V_s - V_o}{L} \tag{7}$$

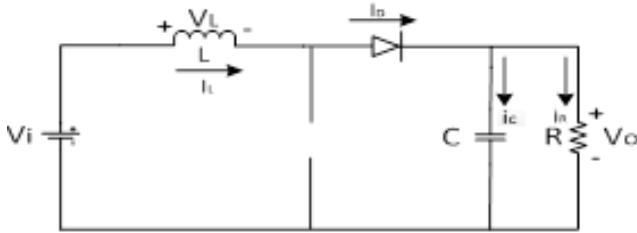


Figure 10. OFF State circuit diagram.

4. Proposed Design Boost Converter for PV Application

The designed configuration and operation of the proposed DC-DC step-up converter are connected to the PV application. Due to the low voltage generated in a PV cell, several PV cells are connected in series (for high voltage) and in parallel (for high current) to form a PV module for the desired output. The IV and PV for irradiance are 1000 [w/m] with a temperature at 50°C.

4.1 Perturb and Observe P&O

Flow chart in Figure 11. presents Perturb and Observe algorithm in the P&O MPPT. Algorithm P&O MPPT has been utilised in the industry attributable to its simplicity of usage. If the operating voltage of configuration PV is perturbed in a provided guidance and $dP/dV > 0$, the perturbation is recognised for moving the operating configuration towards point the MPP. The P&O algorithm would then continue to perturbing in the same orientation that is the PV voltage configuration. If $dP/dV < 0$, at that point the adjustment in the operating point moves the PV configuration away from the MPP, and the P&O algorithm inverts the orientation of the perturbation. The procedure is repeated intermittently to bringing about the system to oscillate on the MPP as appeared in Figure 12. Besides, the oscillation can be decreased via reduction of the perturbation step size. Table 1. summarises the algorithm and presents flow chart for the P&O algorithm of the MPPT.

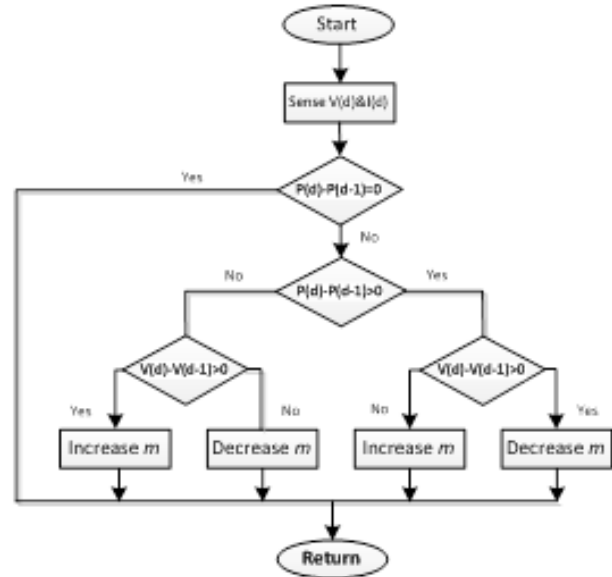


Figure 11. Flowchart of P&O MPPT Algorithm.

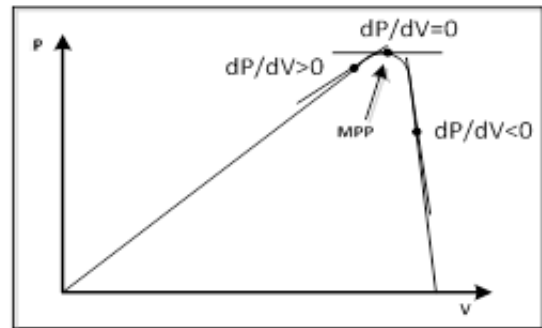


Figure 12. Sign of the dP/dV at various positions on the Power characteristic curve.

Table 1. Algorithm Summary of P&O MPPT

Perturbation	Change in power	Next Perturbation
+	+	+
+	-	-
-	+	-
-	-	+

The new value of M is then multiplied with the reference current I_{ref} obtained by sending the grid voltage V_g before converting to I_{ref} .

$$I_{ref} = V_g x m \tag{8}$$

4.2 Step-up Boost Converter

An operated design of boost converter in CCM to step-up voltage of a oscillate solar panel voltage to a constant high

voltage output of 70 V. The range of duty cycle is between 0-65 percent due to the instability caused via the parasitic components. The proposed design for specification of the relation between input voltage and load voltage is given by:

$$D = \frac{d}{d + 1} \tag{1}$$

$$V_o = V_s / (1-D) \tag{2}$$

Where,

V₀ = Output voltage in volts

V_s= Supply voltage in volts

D= Duty ratio

For producing voltage output to stable, as feedback voltage is utilised using control system. The measure output voltage from control system is compared with a reference voltage and utilised, and the value is various to generate a PWM signal. Based on PWM signal, the change value of duty cycle will be able to change voltage output. To create a signal PWM, was utilised a microcontroller. A (DSP) TMS320F2812 was chosen as it has a progressive approach of the analog to-digital converter, comparator, and PWM generator. F=20 kHz with PWM can be created when (DSP) TMS320F2812 changes the frequency reference between 150 MHz to 50Hz. The strategy of voltage control feedback flow chart as shown in Figure 13. is written and loaded into (DSP) TMS320F2812¹⁹.

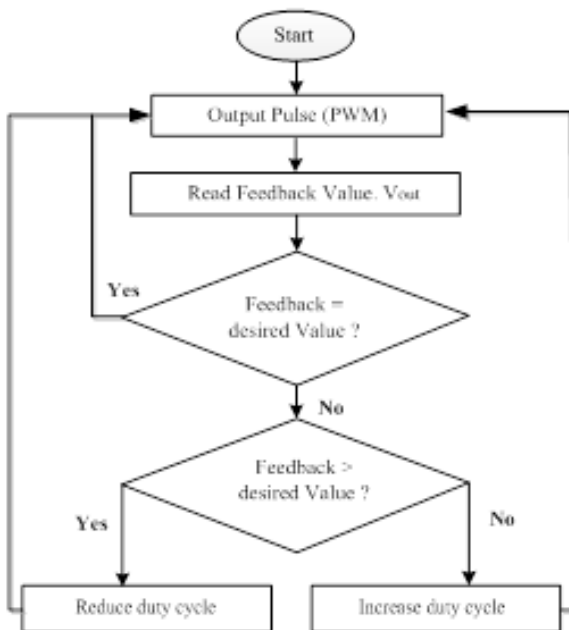


Figure 13. Control flow chart.

The PWM T_m compares the fixed frequency voltage saw-tooth V_{saw} with the control voltage V_c and production the demand duty ratio D. The boost converter plant T_p (s) gives the desirable output voltage V_o conformable to the rectification duty ratio generated by the modulator. The double-lead complete controller can be designed and executed on (DSP) TMS320F2812 control PWM. Figure 14. shows the different equivalent waveforms for voltages and currents.

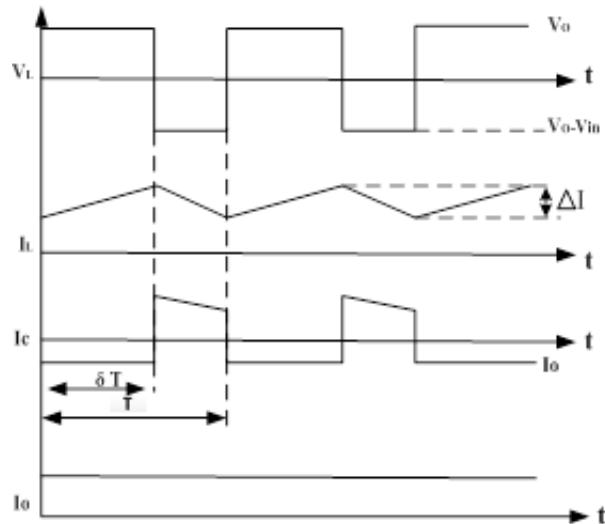


Figure 14. Current and voltage waveforms.

5. Simulation Result

For the simulation result based on MATLAB/SIMULINK, the algorithm for photovoltaic solar coding MPPT was implemented. The DC-DC boost converter system was developed in an environment with different input and output voltage controls by duty cycle 0 - 65% as shown in the complete Simulink diagram in Figure 15. Table 2. shows the parameter for the simulation model.

Table 2. Simulation of Proposed Boost Converter

Components	Value
Power (P)	119.9 W
Voltage Input	24.9-22V
Voltage output	68.5-30V
Duty Cycle	0.65-0.32
Current output	1.75A
Switching Frequency	20 kHz
Capacitor	1000 μF
Inductor	2.07 mH
Load	39Ω

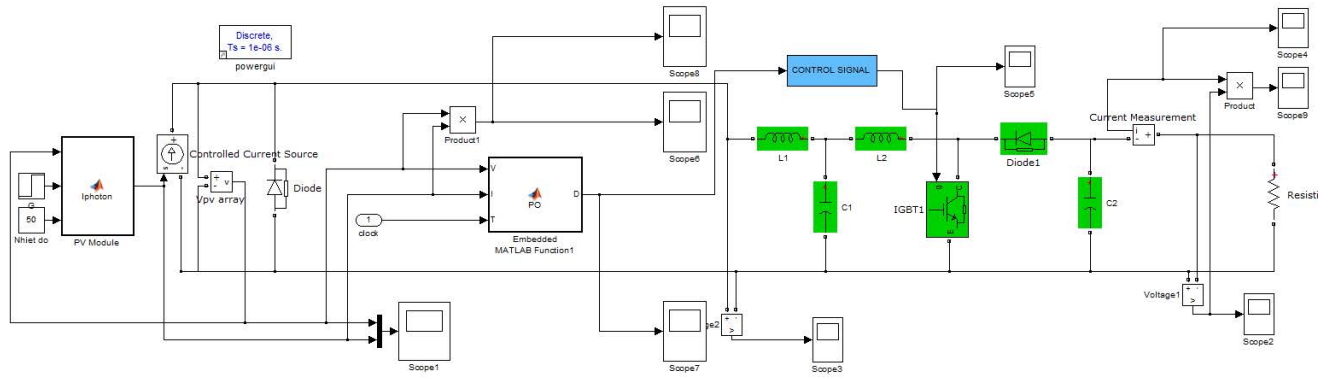


Figure 15. Simulation Model Step-up Boost Converter Based on PV Application.

In Figure 16. presents the duty cycle D equals 0.65, as the proposed simulation results of the converter were able to give an output voltage V_{out} 68.5V at input voltage V_{in} 24.9V. Figure 17. presents the output waveform results for simulation of the boost converter and photovoltaic solar implementation.

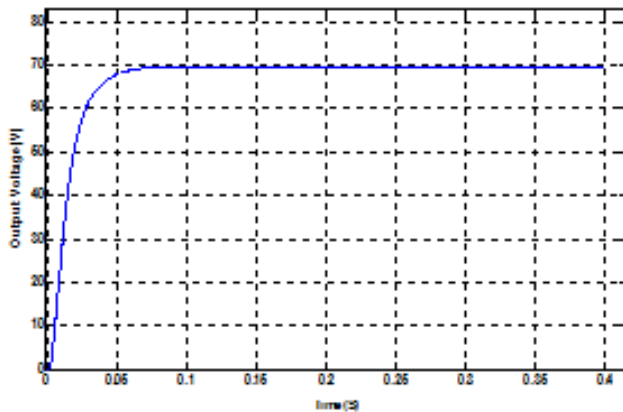


Figure 16. Output Voltage at $D = 0.65$.

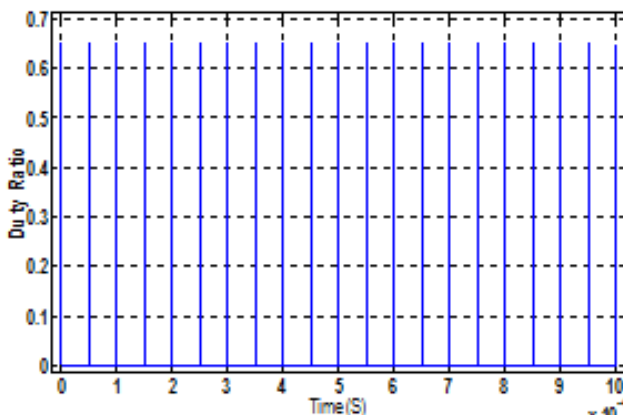


Figure 17. PWM Switching, Duty Cycle (D) = 0.65.

Figure 18. presents output waveform results for simulation of the boost converter and PV solar implementation. In Figure 19. the duty cycle $D = 0.55$ proposed that the converter simulation result was able to give an output voltage V_{out} 51V at input voltage V_{in} 23V.

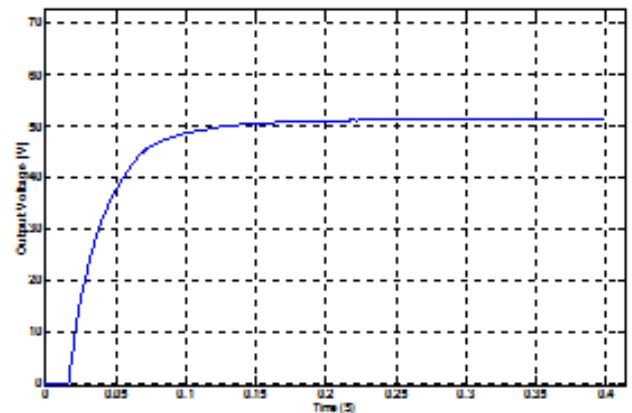


Figure 18. Output Voltage at $D = 0.55$.

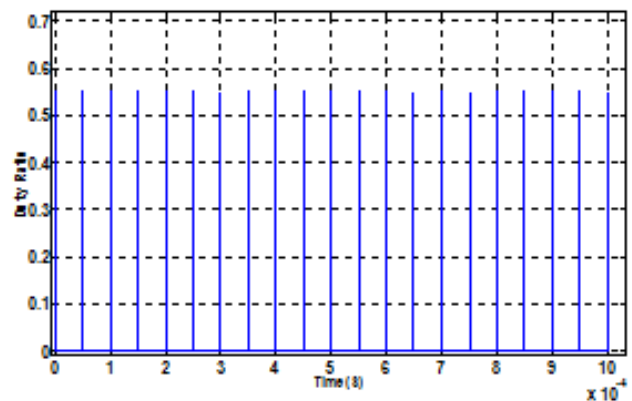


Figure 19. PWM Switching, Duty Cycle (D) = 0.55.

Figure 20. shows the simulation waveform result of the voltage output V_{out} 45V of the PV solar application and boost converter, based on the duty cycle D equals 0.5 as shown in Figure 21. The proposed converter simulation result was able to give an input voltage V_{in} at 23.2V.

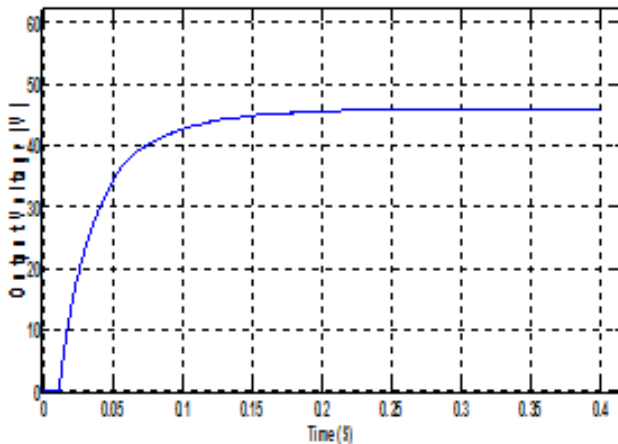


Figure 20. Output Voltage at $D = 0.5$.

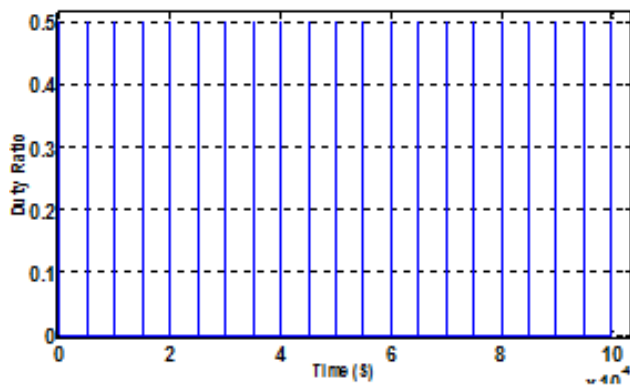


Figure 21. PWM Switching, Duty Cycle (D) = 0.5.

In this Figure 22. , the output voltage waveform for simulation result equal to V_{out} 30V of the PV solar application and boost converter based on duty cycle $D = 0.32$ is shown in Figure 23. The simulation result of the proposed converter was able to give an input voltage V_{in} 22V.

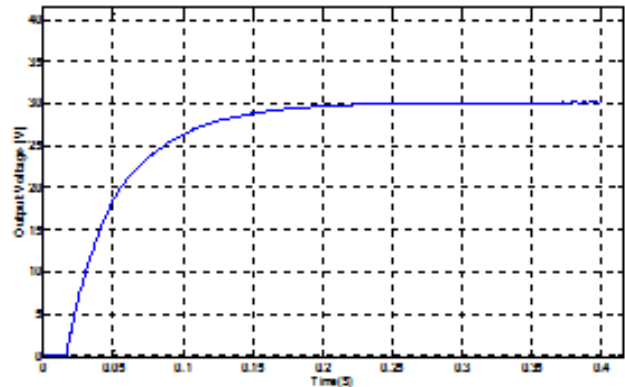


Figure 22. Output Voltage at $D = 0.32$.

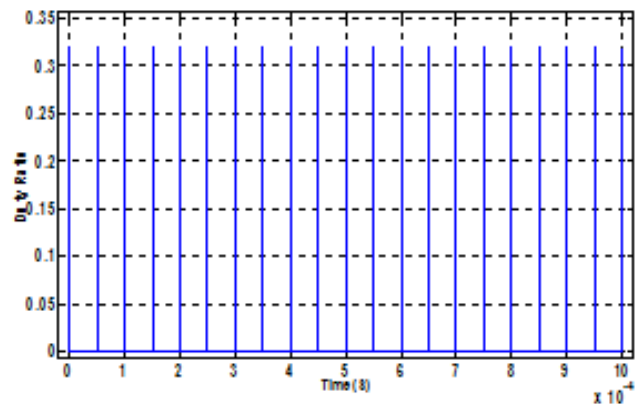


Figure 23. PWM Switching, Duty Cycle (D) = 0.32.

6. Experimental Result

The simulation result was verified experimentally through a laboratory prototype. The latest programmable solar array simulator DC power supply 62000H-S Series provides V_{MPP} 25.0V, I_{MPP} 1.00A, and P_{MPP} 25.00W to the Dc/Dc boost converter as shown in Figure 24. It comprises of a fully control digital signal processing (DSP) TMS320F2812 board generating pulse of the switching signal, an inductor, a diode, a capacitor, and load to greater output voltage from the input voltage.

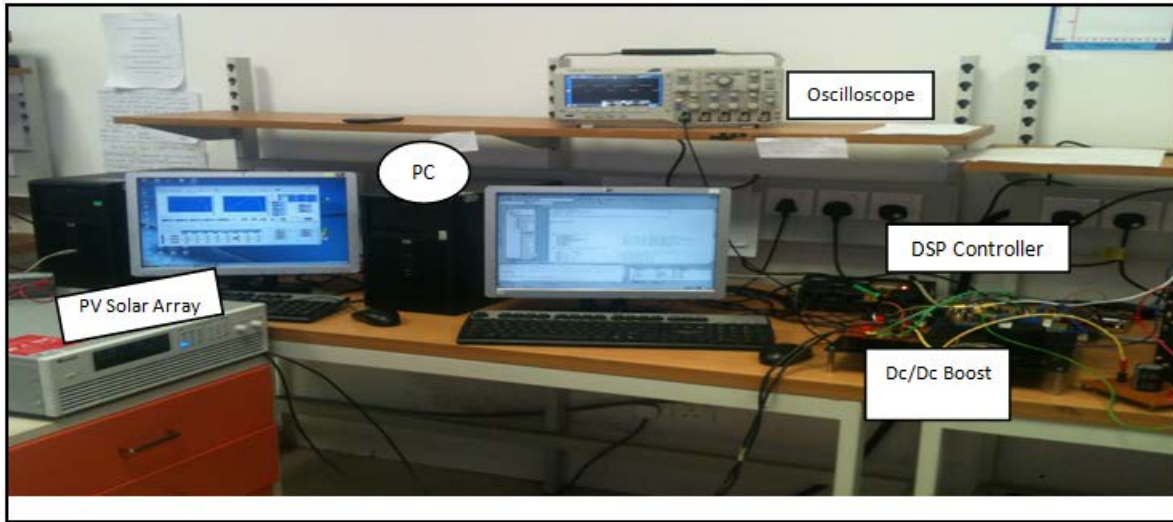


Figure 24. Laboratory hardware Prototype of the overall Proposal System.

For the boost converter circuit, when the transistor is switched on, the input voltage is inspired over the inductor, causing a linear height of current as shown in Figure 25. The output voltage tendentious invert the diode and the capacitor provisions the load current completely. Transistor, the inductor current transfer through the diode, and an invert voltage $V_o - V_{in}$ is inspired over the inductor were not conducted, causing a linear down in the current. An expression for the voltage converter ratio may be obtained by equating the positive and negative volt-seconds on the inductor.

$$V_{in}DT = (V_o - V_{in})(1 - D)T, \text{ giving } \frac{V_o}{V_{in}} = \frac{1}{1 - D} \quad (5)$$

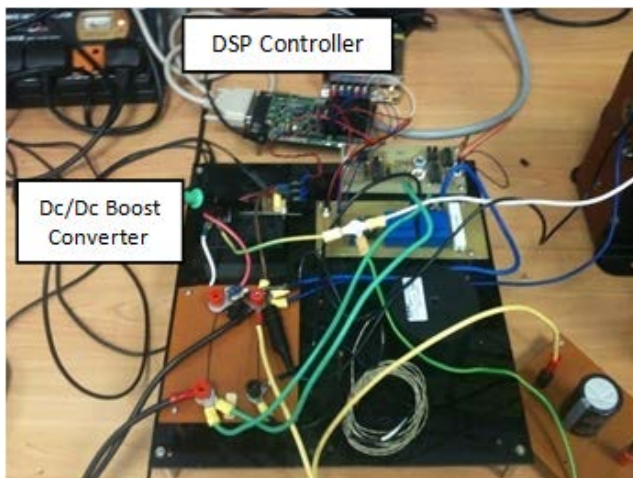


Figure 25. Prototype Dc-Dc Boost Converter.

The prototype of Dc-Dc boost converter hardware was achieved based on duty cycle $D = 0.65$ as shown in Figure 26. Based on input voltage $=V_{in} 26.01V$ the proposed converter experimental results were able to give an output voltage $V_{out} 71.4V$ as shown in Figure 27. This proposal was achieved via the high performance dynamic waveform of the boost converter for PV solar application.

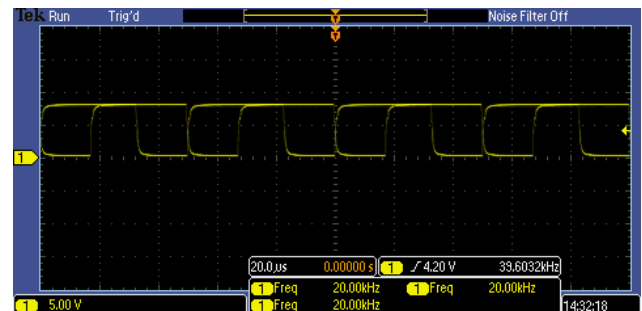


Figure 26. IGBT Switching, Duty Cycle (D) = 0.65.

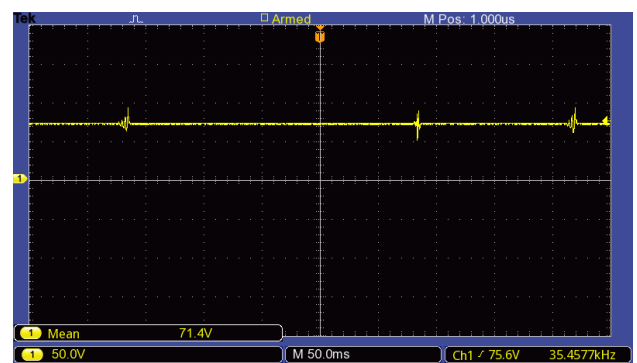


Figure 27. Experiment result of output voltage for D=0.65.

Figure 28. shows the input voltage equals to 26.01V, input current 0.922A and power 23.98W for the experimental result of the PV solar array panel for irradiance 1000W/m2, temperature 50°C, and efficiency 95.91% based on the MPP 50%.

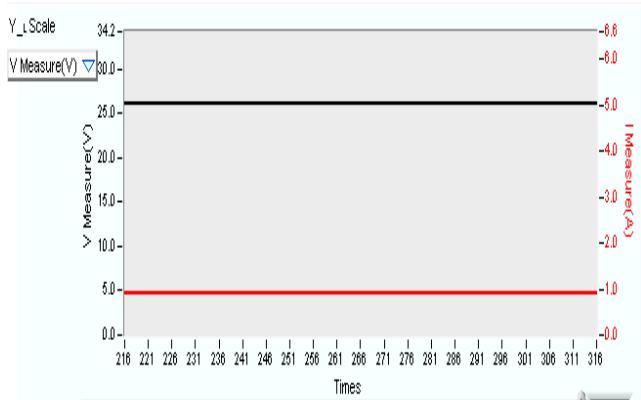


Figure 28. Input voltage and current for PV solar array.

The temperature 50°C and irradiance 1000W/m2 were developed by the simulated curves for I-V and P-V. In Figure 29., the open-circuit voltage Voc 32.08V and short circuit current Isc 1.126A were utilised when the MPP was 25.00W, via PV solar array panel as shown in Figure 30. The proposed experimental verification of the method was set up with the configuration. Based on MPP equal 50% the I-V and P-V curves were programmed into the PV simulator to investigate proposed method of the operation.

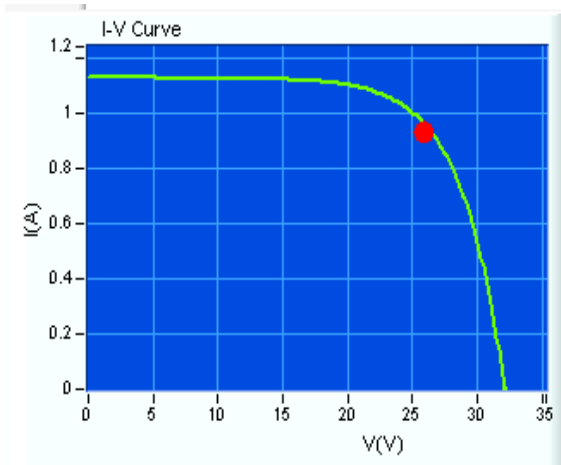


Figure 29. Curve I-V for PV solar array panel MPP 50%.

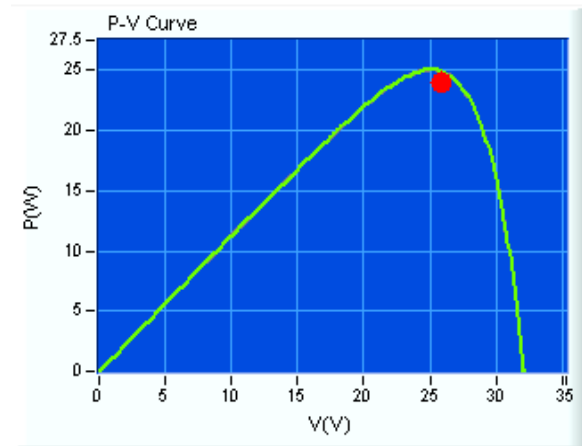


Figure 30. Curve P-V for PV solar array panel MPP 50%.

The Dc/Dc boost converter prototype hardware based on the duty cycle $D = 0.55$ is shown in Figure 31. The experimental results for proposed converter are able to give a V_{out} 52.2V at V_{in} 22.56V as displayed in Figure 32. In this proposal, high performance dynamic waveform of the boost converter for the PV solar application was achieved.

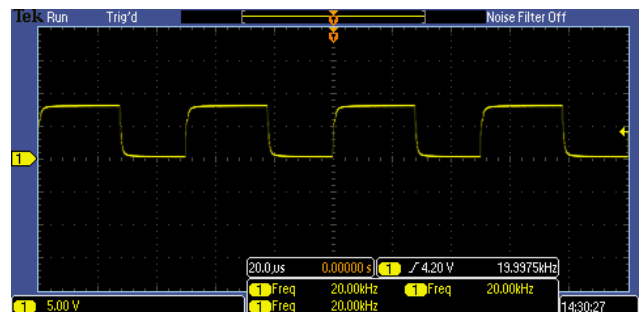


Figure 31. IGBT Switching, Duty Cycle (D) = 0.55.

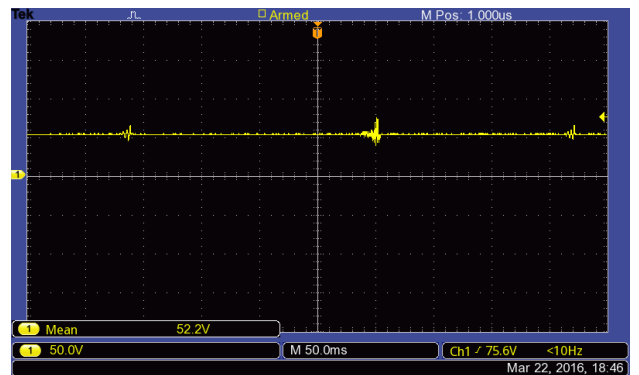


Figure 32. Experiment result of output voltage for $D=0.55$.

For the PV solar array panel experimental result, the input voltage was 22.56V, input current 0.56A, and power 12.7W as shown in Figure 33. For efficiency 94.44% and irradiance 1000W/m², temperature 50°C used was based on the MPP 25%.

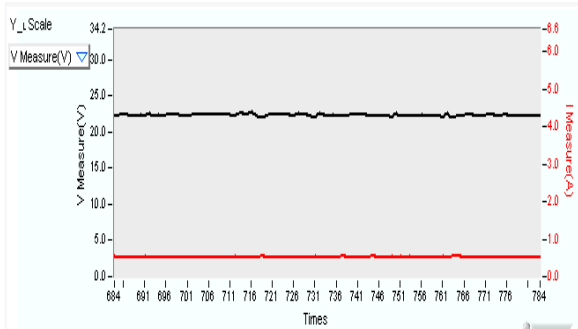


Figure 33. Input voltage and current for PV solar array.

The temperature 50°C and irradiance 1000W/m² were developed by simulated curves for I-V and P-V. In Figure 34, the Voc 32.08V and Isc 0.57A were utilised when the MPP was 12.50W, via PV solar array panel is shown in Figure 35. The proposed experimental verification of the method was set up with the configuration. Based on MPP equal 25%, the I-V and P-V curves were programmed into the PV simulator to investigate proposed method of the operation.

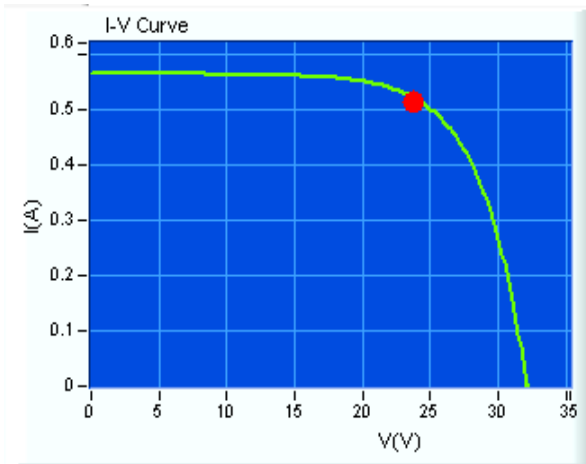


Figure 34. I-V curve for PV solar array panel MPP 25%.

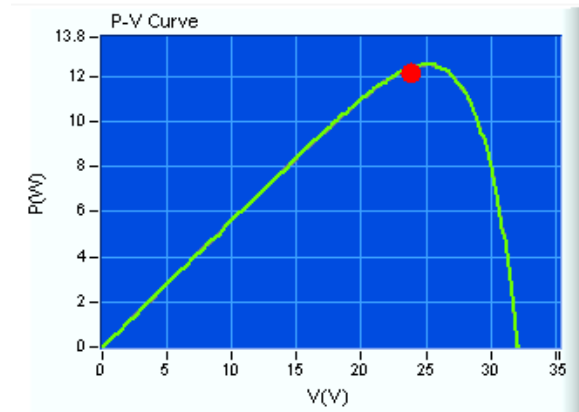


Figure 35. P-V curve for PV solar array panel MPP 25%.

The Dc/Dc boost converter prototype hardware based on the duty cycle $D = 0.5$ is shown in Figure 36. The experimental results for proposed converter are able to give a V_{out} 47.3V at V_{in} 23.4V as presented in Figure 37. In this proposal, high performance dynamic waveform of the boost converter for the PV solar application was achieved.

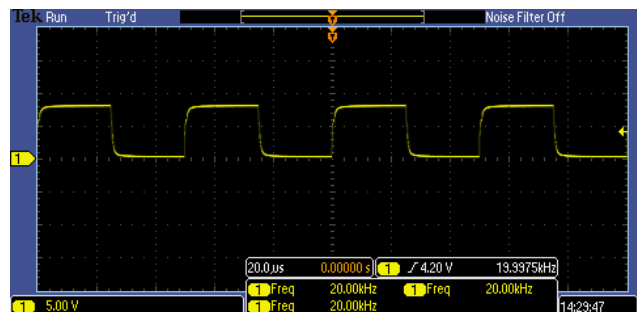


Figure 36. IGBT Switching, Duty Cycle (D) = 0.5.

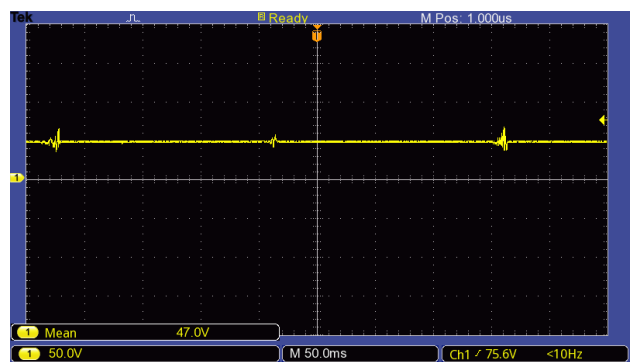


Figure 37. Experiment result of output voltage for D=0.5.

For the PV solar array panel experimental result, the input voltage was 22.27V, input current 0.42A, and power 9.4W are shown in Figure 38. for irradiance 1000W/m², temperature 50C° and efficiency 94.21% based on MPP 20%.

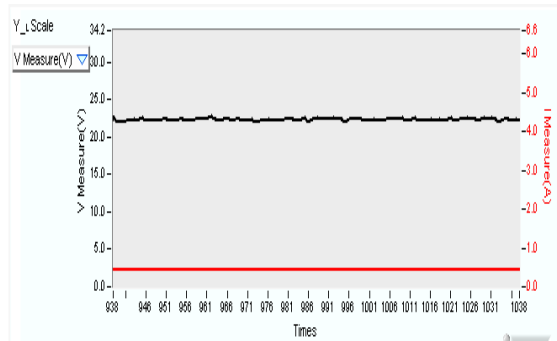


Figure 38. Voltage and current input for PV solar array.

The irradiance 1000W/m² and temperature 50°C were the simulated curves for I-V and P-V. Based on MPP 10.0W the I_{sc} 0.45A and V_{oc} 32.08V as shown in Figure 39. via utilise PV solar array panel is shown in Figure 40. The proposed experimental verification of the method was set up with the configuration. MPP equal to 20% the I-V and P-V curves were programmed into the PV simulator to investigate proposed method of the operation.

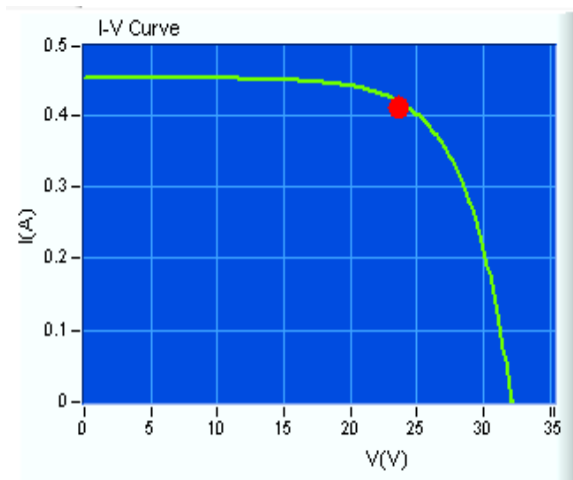


Figure 39. Curve I-V for PV solar array panel MPP 20%.

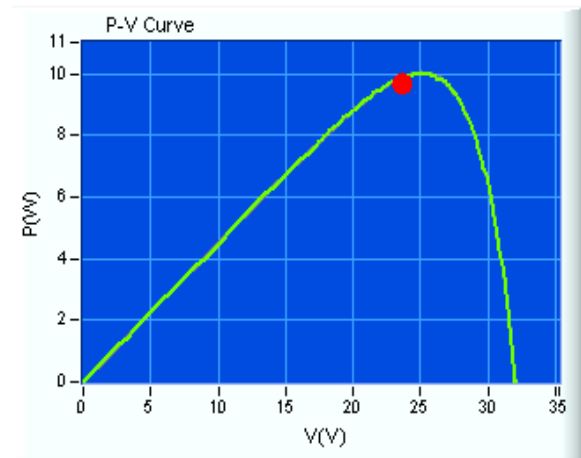


Figure 40. Curve P-V for PV solar array panel MPP 20%.

The Dc/Dc boost converter prototype hardware based on the duty cycle $D = 0.32$ is shown in Figure 41. The experimental results for proposed converter are able to give a V_{out} 33.0V at V_{in} 22.8V as shown in Figure 42. In this proposal, high performance dynamic waveform of the boost converter for the PV solar application was achieved.

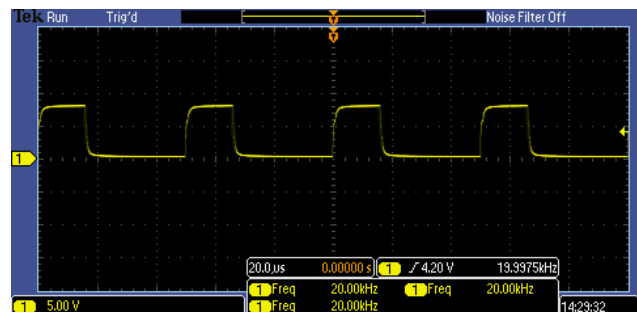


Figure 41. IGBT Switching, Duty Cycle (D) = 0.32.

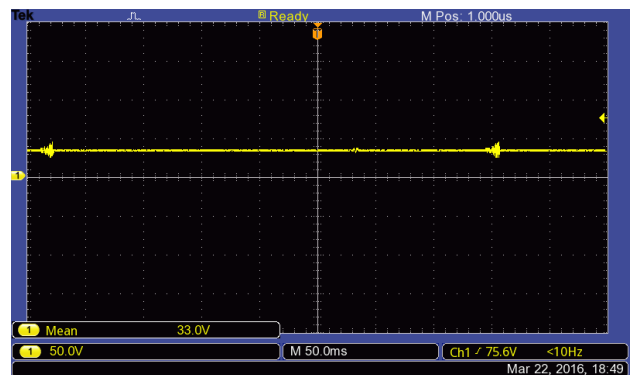


Figure 42. Experiment result of output voltage for D=0.32.

The experimental result of the PV solar array panel, input voltage equal 22.8V, input current 0.21A, and power 4.6W are shown in Figure 43. for irradiance 1000W/m², temperature 50°C and efficiency 91.54% based on MPP 10%.

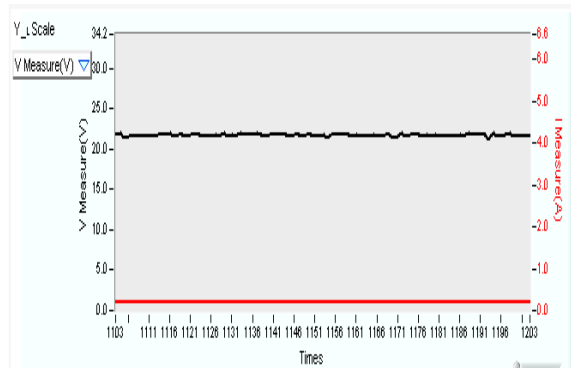


Figure 43. Input voltage and current for PV solar array.

The temperature 50°C and irradiance 1000W/m² was developed via simulated curves for I-V and P-V. Figure 44. presents Voc equal to 32.08V and Isc equal to 0.22A when the MPP was 10.0W via PV solar array panel is shown in Figure 45. The proposed experimental verification of the method was set up with the configuration. Based on MPP equal to 10% the I-V and P-V curves were programmed into the PV simulator to investigate proposed method of the operation.

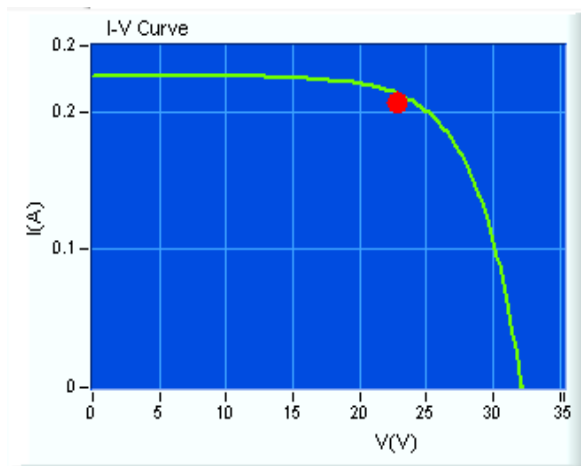


Figure 44. I-V curve for PV solar array panel MPP 10%.

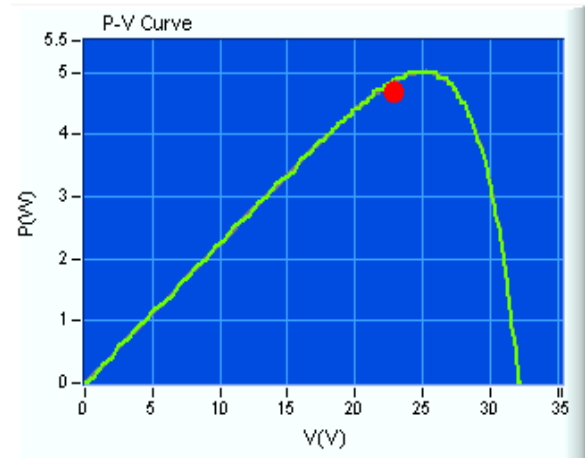


Figure 45. P-V curve for PV solar array panel MPP 10%.

7. Conclusion

In this paper, the hybrid (MPPT) technique and (DSP) TMS320F2812, based on the step-up DC/DC boost converter were verified experimentally through a laboratory prototype for being able to generate a high voltage via simulation result. The feedback path was established by a control circuit such that a proper duty cycle was achieved for the output voltage (V_o) desired for PV application system. The experimental results show that the proposed method can obtain the MPP under various duty cycle D control when the output voltage (V_o) is implemented.

8. Acknowledgment

The authors wish to thank Universiti Teknikal Malaysia Melaka (UTeM) for Fellowship award and Ministry of Higher Education, Malaysia (MOHE) for supporting this research under the grant FRGS/1/2016/TK04/UTEM/02/8.

9. References

1. Mohammed. Rasheed, Rosli. Omar, Afy. Sabari, and Ma-

- rizan. Sulaiman. Validation of a three-phase cascaded multilevel inverter based on Newton Raphson (N . R .). May 2016; 9(20) 1–13.
2. Mohammed. Rasheed, Rosli. Omar, and Marizan. Sulaiman. Harmonic reduction in multilevel inverter based on super capacitor as a storage. TELKOMNIKA Indones. J. Electr. Eng. December 2015; 16(3): 520–30.
 3. Hasaneen B.M. and Adela. Elbaset Mohammed. Design and simulation of DC/DC boost converter." 2008. 12th Int. Middle-East Power Syst. Conf. Mar. 2008; p. 335–40.
 4. Kotak V C and Preti P. Tyagi. DC To DC Converter in Maximum Power Point Tracker. International Journal of Advanced Research in Electrical, Electronics and Instrumentation Engineering. December 2013; 2(12): 6115–25.
 5. Rosas-caro J.C., Ramírez J.M, and. García-vite P. M. Novel High Efficiency Multilevel DC-DC Boost Converter Topologies and Modulation Strategies G. Cinvestav IPN. 2008; 2146–51.
 6. Butti G and Biela J., Novel High Efficiency Multilevel DC-DC Boost Converter Topologies and Modulation Strategies. Newave SA, Research and Development Department. Via Luserte Sud 9 CH-6572 Quartino. Power Electronics and Applications (EPE 2011), Proceedings of the 2011-14th European Conference on. 2011; p1-10.
 7. Kavita Goswami, Bishwajeet Pandey , Akbar Hussaian D M. , Tanesh Kumar and Kartik Kalia. Input / output buffer based vedic multiplier design for thermal aware energy efficient digital signal processing on 28nm FPGA. Indian Journal of Science and Technology. March 2016; 9(10):1–8.
 8. Rosli. Omar, Mohammed. Rasheed, Marizan. Sulaiman, and M. Room. Tamijis, Modeling and simulation of a three phase multilevel inverter for harmonic reduction based on modified space vector pulse width modulation (SVPWM). Journal of Theoretical & Applied Information Technology. 2015; 77(2):178-189
 9. Julio C. Rosas-Caro, Juan M. Ramírez, Pedro Martín. A DC-DC multilevel boost converter. IET Power Electronics. 2010; 3(1): 129.
 10. Babu G.H., Anuhya AV, and Venkatram N. Digital Signal Processing Scheme for Open Loop and Closed Loop IFOG using MATLAB / SIMULINK. Indian Journal of Science and Technology. March 2016; 9(11): 1-10.
 11. Vinayaka B C. and Prasad S N. Modeling and design of five level cascaded h-bridge multilevel inverter with DC / DC boost converter. International Journal of Engineering Research and Application. June 2014; 4(6): 50–55.
 12. Kyung Ki Kim. Simple CNFET digital circuit design using Back-gate Voltages. Indian Journal of Science and Technology. April 2016; 9(16):1-6. [13]
 13. Anand R. and Gnanambal I. Modeling and analysis of cascade multilevel DC-DC boost converter topologies based on H-bridge switched inductor. Research Journal of Applied Sciences, Engineering and Technology. 2015; 9(3):145–57.
 14. Abhimanyu Bhimarjun Panthee and Muralidhar M. An advanced five level cascaded inverter based power conditioning system for solar power applications. International Journal of Engineering Research and Technology. August 2014; 3(8): 609–14.
 15. Pal S., Dalapati S. and Processors D. S., "Digital simulation of two level inverter based on space vector pulse width modulation. Indian Journal of Science and Technology. Apr 2012; 5(4): 2557–68.
 16. Mostafa SMG. Designing a oost Inverter to interface between photovoltaic system and power utilities. IOSR J. Electr. Electron. Eng. 2012.; 3(2) 01–06.
 17. Ravi Srikanth G., Achyuth Charan K Mowmin A., Syed Baji1 SK, Gopi Latha V., Md. Majhar Hussain. A Grid connected hybrid asymmetrical nine level inverter topology using boost converter. IOSR Journal of Engineering. Apr. 2012; 2(4):900–07.
 18. Arathy M, Sreekala P, "Design and implementation of A PV powered five level inverter using multilevel differential boost converter. International Journal of Advanced Research in Electrical, Electronics and Instrumentation Engineering. June 2014; 3(6):10315–20.
 19. Pui-Weng Chan, Syafrudin Masri. DC-DC boost converter with constant output voltage for grid connected photovoltaic application system. Industrial Electronic Seminar. 2010;